doi:10.1093/brain/awr326 Brain 2012: 135; 62–71 | 62

BRAIN
A JOURNAL OF NEUROLOGY

Sensory neuronopathy in patients harbouring recessive polymerase γ mutations

Nichola Z. Lax,[1,2] Roger G. Whittaker,[1,3] Philippa D. Hepplewhite,[1] Amy K. Reeve,[1,2] Emma L. Blakely,[1] Evelyn Jaros,[4,5] Paul G. Ince,[6] Robert W. Taylor,[1] Peter R. W. Fawcett[3] and Doug M. Turnbull[1,2]

1 Mitochondrial Research Group, Institute for Ageing and Health, Newcastle University, Framlington Place, Newcastle upon Tyne, NE2 4HH, UK
2 Newcastle University Centre for Brain Ageing and Vitality, Institute for Ageing and Health, Newcastle University, Framlington Place, Newcastle upon Tyne, NE2 4HH, UK
3 Department of Clinical Neurophysiology, Royal Victoria Infirmary, Queen Victoria Road, Newcastle upon Tyne, NE1 4LP, UK
4 Neuropathology/Cellular Pathology, Royal Victoria Infirmary, Queen Victoria Road, Newcastle upon Tyne, NE1 4LP, UK
5 Institute for Ageing and Health, Newcastle University, Campus for Ageing and Vitality, Newcastle upon Tyne, NE4 5PL, UK
6 Department of Neuroscience, Sheffield Institute for Translational Neuroscience, University of Sheffield, 385a Glossop Road, Sheffield, S10 2HQ, UK

Correspondence to: Prof. Doug M. Turnbull,
Mitochondrial Research Group,
The Medical School,
Newcastle University,
Newcastle upon Tyne,
NE2 4HH, UK
E-mail: doug.turnbull@newcastle.ac.uk

Defects in the mitochondrial DNA replication enzyme, polymerase γ, are an important cause of mitochondrial disease with ~25% of all adult diagnoses attributed to mutations in the *POLG* gene. Peripheral neuronopathy is often part of the clinical syndrome and can represent the most disabling feature. In spite of this, the molecular mechanisms underlying the neuronopathy remain to be elucidated and treatment strategies are limited. In the present study, we use a combined approach comprising clinical, electrophysiological, neuropathological and molecular genetic investigations to unravel the mechanisms underpinning peripheral neuronopathy in autosomal recessive polymerase γ-related disease. Electrophysiological assessments documented a dorsal root ganglionopathy in all 11 cases. Of the 11 cases, eight also showed changes consistent with motor fibre loss. Detailed neuropathological investigation of two patients confirmed the electrophysiological findings, revealing atrophy of posterior columns and striking neuronal cell loss from the dorsal root ganglia, which was accompanied by severe mitochondrial biochemical abnormalities involving respiratory chain complexes I and IV due to clonally-expanded mitochondrial DNA deletions and a significant reduction in mitochondrial DNA copy number in affected neurons. We propose that the respiratory chain defects, secondary to mitochondrial DNA deletion and depletion, are likely to be responsible for pathology observed in the dorsal root ganglion and the sensory ganglionopathy documented electrophysiologically.

Keywords: polymerase γ; mitochondrial DNA; sensory neuronopathy; neurodegeneration

Abbreviations: CNPase = 2′,3′ cyclic nucleotide 3′ phosphodiesterase; COX = cytochrome *c* oxidase; POLG = polymerase γ

Received August 23, 2011. Revised October 7, 2011. Accepted November 6, 2011. Advance Access publication December 20, 2011

Introduction

The 16 569 base pair mitochondrial genome is replicated and maintained by the nuclear encoded mitochondrial DNA polymerase γ (POLG) (Clayton, 1982). The POLG protein forms a heterotrimer consisting of a large catalytic subunit containing polymerase and exonuclease activities and two smaller 55 kDa accessory subunits that enhance processivity. The catalytic domain of the POLG protein is encoded by the *POLG* gene located on chromosome 15q25 (MIM# 174763). Over 150 pathogenic mutations have been described in the *POLG* gene and are associated with a broad range of clinical phenotypes, some of which are inherited in an autosomal-dominant manner and others that are autosomal recessive. *POLG* mutations cause a spectrum of neurodegenerative diseases ranging from Alpers–Huttenlocher syndrome in infancy (Naviaux and Nguyen, 2004), to a mitochondrial encephalopathy with lactic acidosis and stroke-like episodes (MELAS)-type presentation in middle age (Deschauer *et al*., 2007), to mitochondrial recessive ataxic syndrome (MIRAS) with an onset ranging from adolescence to middle-age defined by ataxia, peripheral sensory neuropathy and epileptic seizures (Rantamaki *et al*., 2001; Van Goethem *et al*., 2004; Hakonen *et al*., 2005; Winterthun *et al*., 2005) and late-onset chronic progressive ophthalmoplegia. It is not clear what causes such variability in clinical phenotype; however, recent studies suggest that the site of the mutation (Horvath *et al*., 2006; Tzoulis *et al*., 2006) or involvement of epigenetic factors (Stricker *et al*., 2009) might be important in the development of certain symptoms.

Although patients with autosomal recessive POLG deficiency may present with diverse neurological symptoms, sensory neuronopathy is a common feature and in some cases the presenting feature (Fadic *et al*., 1997; Van Goethem *et al*., 2003). Clinically, patients may present with loss of position sense, glove and stocking numbness and impaired vibration sensation (Filosto *et al*., 2003). In most patients with POLG deficiency, motor symptoms are mild, with sensory symptoms the major feature (Tzoulis *et al*., 2006; Schicks *et al*., 2010). The neuronopathy can be the dominating feature, with severe sensory ataxia associated with dysarthria and ophthalmoparesis in the so-called SANDO (sensory ataxia associated with dysarthria and ophthalmoparesis) syndrome (Van Goethem *et al*., 2003, 2004; Winterthun *et al*., 2005; Gago *et al*., 2006). This tends to be progressive and leads to marked disability in some patients.

In view of the importance of the peripheral neuronopathy in POLG deficiency, we have performed a detailed clinical, neurophysiological, genetic and pathological study of the neuronopathy seen in patients harbouring autosomal recessive *POLG* mutations. Clinical and electrophysiological findings show peripheral neuronopathy is part of the clinical syndrome in patients harbouring *POLG* defects. Typically, electrophysiological investigation reveals reduced sensory nerve action potentials with preserved conduction velocity, suggestive of dorsal root ganglion dysfunction. Motor fibre loss is also seen, but tends to occur later in the disease process. Neuropathological investigation supports our nerve conduction studies by showing that the main abnormality is severe respiratory chain deficiency and neuronal cell loss in the dorsal root ganglia due to mitochondrial DNA depletion and accumulation of mitochondrial DNA deletions.

Patients and methods

Clinical examination and neurophysiological studies

In total, 11 patients (Patients 1–11) with autosomal recessive *POLG* mutations who were of European origin from Northern England (seven male, four female, age range 18–61 years) underwent clinical and neurophysiological assessment for this study. Unfortunately, formal nerve conduction studies or concentric needle EMG were not performed on Patient 12 although she displayed symptoms of neuropathy and her neuropathology is described here. Analysis of muscle biopsy samples revealed secondary mitochondrial DNA changes in every patient, with evidence of mitochondrial DNA deletions in association with focal cytochrome *c* oxidase (COX) deficiency. In five patients, clinical evidence of peripheral neuronopathy was documented at first presentation. In the remainder, symptoms and signs of neuronopathy developed between 1 and 14 years later (mean 6.8 years). Associated clinical features are given in Table 1. None of the patients had diabetes or other causes of neuropathy.

Motor nerve conduction studies were performed on median, ulnar, common peroneal and tibial nerves and sensory studies on radial, median, ulnar, sural and superficial peroneal nerves. Concentric needle EMG was performed in 10 patients in a variety of upper and lower limb muscles depending on clinical presentation. Macro-EMG was performed in two patients.

Sensory axonal neuropathy was defined as reduction in sensory nerve action potentials with amplitudes of $<50\%$ of normal values with a conduction velocity $>70\%$ of normal values. Sensory neuronopathy was defined on the basis of parallel reduction in amplitude in both proximal and distal nerve segments. Motor neuronopathy was defined as neurogenic change in proximal and distal muscles. Myopathy was defined as the presence of short duration, low amplitude motor units with early recruitment on concentric needle EMG.

All human studies were approved and performed under the ethical guidelines issued by Newcastle University, with written informed consent obtained from the patient.

Neuropathological studies

Patient details

We characterized the neuropathological features of a clinically and genetically well-defined 50-year-old (Patient 3) and a 24-year-old patient (Patient 12). Patient 3 first presented in young adulthood with slurred speech, problems with balance, increasing fatigue and jerky uncontrolled movements of the limbs. As his disease progressed, he developed bilateral ptosis, progressive external ophthalmoplegia and became severely ataxic. A diagnostic muscle biopsy revealed COX-deficient fibres and multiple mitochondrial DNA deletions, with molecular investigations confirming the presence of compound heterozygous (p.A467T and p.X1240Q) *POLG* mutations. Detailed neuropathological changes in this patient have been described previously (Cottrell *et al*., 2000). Patient 12 presented at 20 years of age with epileptic seizures following pregnancy. Over the subsequent 4 years until her death, she developed a progressive ataxia with epilepsy, paraparesis and cognitive decline. Muscle biopsy revealed no histochemical

Table 1 Clinical and molecular characterization of the patient cohort

Patient	Sex	Age of disease onset (years)	Age at study (years)	Primary clinical features						Muscle histochemistry		Molecular defects		Nerve conduction studies	
				CPEO	Ptosis	Peripheral neuropathy	Ataxia	Dysarthria	Epilepsy	COX-deficient fibres (%)	RRF (%)	*POLG* mutation	Presence of mitochondrial DNA deletions	NCS interpretation	EMG
1	M	17	42	+	+	+				20	20	p.A467T; p.R1096C	Confirmed	Sensory and motor neuronopathy	Distal and proximal neurogenic change
2	M	18	36	+	+	+				10	5	p.A467T; p.A467T	Confirmed	Severe sensory and moderate motor neuronopathy. Proximal myopathy.	Distal neurogenic change, proximal myopathy
3[a]	M	18	50	+	+	+	+			20		p.A467T; p.X1240Q	Confirmed	Severe sensory neuronopathy	Not investigated
4	F	22	61	+	+	+	+	+		6		p.A862T; p.R1047W	Confirmed	Axonal sensory neuropathy / neuronopathy	Distal and proximal neurogenic change
5	M	25	49	+	+	+			+	16	5	p.W748S; p.R1096C	Confirmed	Severe sensory and moderate motor neuronopathy	Distal neurogenic change, proximal myopathy
6	M	26	36	+		+	+	+		3		p.G746S; p.G484S	Confirmed	Severe sensory and moderate motor neuronopathy	Distal and proximal neurogenic change
7	M	34	47	+	+	+				5	5	p.A467T; p.W748S	Confirmed	Severe sensory and moderate motor neuronopathy	Distal neurogenic change, proximal myopathy
8	F	41	42	+	+	+			+	25	5	p.A467T; p.X1240Q	Confirmed	Sensory and motor neuronopathy	Distal neurogenic change
9	M	41	44	+	+	+				10		p.A467T; p.A467T	Confirmed	Severe sensory and moderate motor neuronopathy. Proximal myopathy.	Distal and proximal neurogenic change
10	F	44	48	+	+	+	+			5		p.A467T; p.W748S	Confirmed	Severe sensory, moderate motor axonal neuronopathy	Distal neurogenic, proximal myopathy
11	F	16	18			+	+		+	2		p.A467T; p.W748S	Confirmed	Moderate sensory neuronopathy	Normal
12[a]	F	20				+	+		+			p.A467T; p.W748S	Confirmed	Not investigated.	Not investigated.

a The cases used for post-mortem neuropathological investigation.
CPEO = Chronic Progressive External Ophthalmoplegia; NCS = nerve conduction study; RRF = ragged-red fibres.

evidence of either a metabolic myopathy or mitochondrial disorder; however, molecular genetic diagnosis confirmed the presence of the recessive p.A467T and p.W748S *POLG* mutations.

Fixed and frozen spinal cord (at the cervical, thoracic, lumbar and sacral levels) and dorsal root ganglia tissues were obtained from Patient 3, whereas only fixed spinal cord tissues were obtained from Patient 12 and could only be assessed using general neurohistopathological stains since the length of fixation affected sensitivity of primary antibodies (Table 1). This tissue was acquired from the Newcastle Brain Tissue Resource and the Sheffield Brain Tissue Bank. All control cases were matched with our patients for age, sex, post-mortem interval and length of tissue fixation. Ethical approval and full consent was granted for this work.

Tissue preparation and immunohistochemistry

Routine histochemistry using cresyl fast violet, haematoxylin and eosin, Loyez stain and Bielschowsky's silver stains were performed on formalin-fixed paraffin-embedded spinal cord (including cervical, thoracic, lumbar and sacral levels), lower medulla, sympathetic and dorsal root ganglion tissues.

Immunohistochemical staining was performed using a range of primary antibodies (Supplementary Table 1); these included markers to assess mitochondrial density (anti-porin), components of the mitochondrial respiratory chain (complex I: anti-CI-8, anti-CI-15, anti-CI-19, anti-CI-20, anti-CI-30, anti-CI39; complex II: anti-CII-70; complex IV: anti-COX-I and anti-COX-IV), axons (anti-SMI31 and SMI-32), myelin components [anti-myelin basic protein and anti-2′,3′ cyclic nucleotide 3′ phosphodiesterase (CNPase) and astrocytes (anti-glial fibrillary acidic protein)]. Briefly, immunohistochemical staining involved cutting and mounting 5 μm formalin-fixed paraffin-embedded sections on to SuperFrost™ Plus slides (VWR International). Sections were then deparaffinized in two changes of Histo-Clear (National Diagnostics) and rehydrated through an ethanol series (2 × 100% for 5 min each; 95% for 5 min; 70% for 5 min), before rinsing in distilled water. Antigen retrieval was then performed to aid unmasking of the antigens according to the methods described in Supplementary Table 1. The sections were then incubated in a 3% solution of hydrogen peroxide to block endogenous peroxide for 20 min and incubated with the appropriate antibody dilution in Tris-buffered saline (Supplementary Table 1) for 1 h at room temperature. This was followed by three 5 min washes with Tris-buffered saline and then the polymer detection system (Menarini Diagnostics) was used. This involved the recognition of the mouse or rabbit epitope of the primary antibody with incubation of a Universal probe for 30 min at room temperature. The sections were washed 3 × 5 min with Tris-buffered saline and horseradish peroxidase-polymer was added to amplify the primary antibody signal. The sections were washed well with water and visualized with 3,3′-diaminobenzidine (DAB; Sigma) and a haematoxylin (Raymond A. Lamb) counterstain. The sections were then dehydrated and mounted in DPX.

Neuronal cell counting

In order to establish the degree of neuronal cell loss in Patient 3, both spinal cord and dorsal root ganglion tissues were processed using the cresyl fast violet stain on 20 μm tissue sections. Specifically, one section was taken from each spinal cord case due to limited tissue availability and three sections from each case containing dorsal root ganglia separated by a thickness of 100 μm. Analysis of neuronal density was then performed using a stereological workstation with a modified light microscope (Olympus), motorized stage for automatic sampling, CCD colour video and stereology software (Stereo Investigator, MBF Bioscience). The spinal cord was outlined and divided into anterior and posterior regions and the entire dorsal root ganglia outlined at a low magnification (×2) and following this, a meander scan at ×40 magnification was initiated throughout the region of interest and each neuron with a visible nucleolus and cell body profile was counted. A density was then derived by dividing the total number of neurons by the area sampled, then multiplying this figure by the thickness of the sections.

Mitochondrial enzyme histochemistry, laser capture micro-dissection of cells and quantitative real-time polymerase chain reaction

Mitochondrial changes were assessed in all tissue samples by sequential COX/succinate dehydrogenase histochemistry as previously described (Betts *et al*., 2006). For laser micro-dissection of single neurons, 20 μm cryostat sections were mounted on polyethylene naphthalate membrane slides (Leica Microsystems), subjected to sequential COX/succinate dehydrogenase or succinate dehydrogenase only histochemistry and air-dried following ethanol dehydration. Single neurons were cut into sterile 0.5 ml polymerase chain reaction tubes using a Leica Laser Microdissection System (AS-LMD 6000, Leica Microsystems) and lysed overnight (Taylor *et al*., 2003). A real-time polymerase chain reaction assay using specific fluorogenic TaqMan® probes (Applied Biosystems) was employed to determine the relative amplification of mitochondrial DNA within the *MT-ND1* and *MT-ND4* genes (He *et al*., 2002; Krishnan *et al*., 2007). Single-cell lysates derived from succinate dehydrogenase-stained slides only were examined in triplicate and mitochondrial DNA deletion level was determined from the proportion of wild-type (*MT-ND4*) to total copy number (*MT-ND1*), using the established ΔCt method (He *et al*., 2002). To determine the wild-type levels of mitochondrial DNA, a standard curve of known *MT-ND4* copy number was generated from template DNA, which allowed the determination of the number of copies of *MT-ND4* present within dorsal root ganglia neurons. This value was then corrected to calculate copy number per unit area (μm^2).

Results

Neurophysiology

The clinical features and nerve conduction assessments of all 11 patients are presented in Table 1. All patients showed evidence of a sensory neuronopathy. Five patients presented with sensory ataxia, three with electrophysiological features of a pure sensory neuronopathy, two also had evidence of motor fibre involvement. In one of these patients, this initial presentation with ataxia was as part of a rapidly progressive clinical course with multiple stroke-like episodes and intractable seizures. Progressive external ophthalmoplegia and ptosis were also a common finding in all patients.

The remaining six patients developed peripheral neuronopathy later in their disease, and showed a mixture of sensory and motor fibre involvement. In two of these patients, macro-EMG showed increased fibre density and median macro motor unit potential amplitude, consistent with a motor neuronopathy. Four patients showed additional evidence of a proximal myopathy on concentric needle EMG (Table 1).

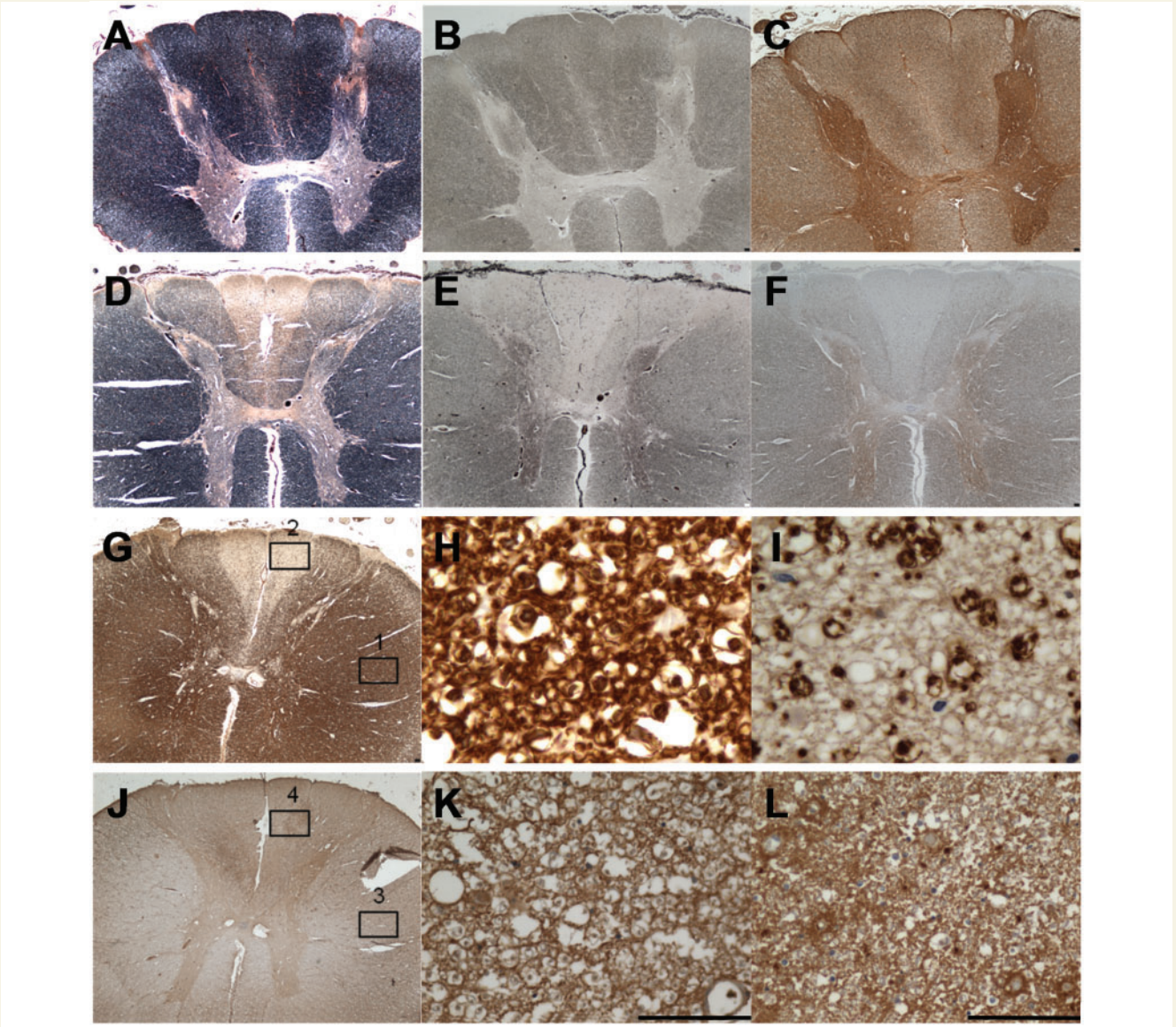

Figure 1 Posterior column degeneration in Patient 3 is characterized by severe loss of myelin and axons. (**A–C**) Control spinal cord: intact myelin in all white matter funiculi. (**A**) Loyez stain, (**B**) Bielschowsky's silver stain and (**C**) SMI31 immunohistochemistry. (**D**) Patient 3 spinal cord: myelin loss is severe in the fasciculus gracilis and moderately severe in fasciculus cuneatus of the posterior spinal funiculus (Loyez). (**E** and **F**) Patient 3 spinal cord: axon loss is severe in the fasciculus gracilis and moderately severe in fasciculus cuneatus of the posterior spinal funiculus (Bielschowsky's stain in **E** and SMI31 immunohistochemistry in **F**). (**G**) Patient 3 spinal cord: myelin basic protein immunohistochemistry shows a similar degree of myelin loss in the posterior spinal funiculus as Loyez (**D**). (**H**) Patient spinal cord, magnified region in Box 1 (lateral funiculus) of **G**: normal myelinated fibre density in the intact spinal cord (myelin basic protein immunohistochemistry). (**I**) Patient spinal cord magnified region in Box 2 of **G**: severe loss of myelinated fibres in the affected fasciculus gracilis (myelin basic protein immunohistochemistry). (**J**) Patient 3 spinal cord: the density of oligodendrocytes in the affected posterior funiculus is higher from that in the unaffected lateral funiculus (CNPase immunohistochemistry). (**K** and **L**) Patient spinal cord magnified regions in Box 3 (from lateral funiculus) and in Box 4 (from fasciculus gracilis). Scale bars = 100 μm.

Neuropathological studies

Neurohistopathological findings

Neurohistopathological investigation of the dorsal root ganglia with standard stains showed neuron loss and a reduction in cell body size. Evaluation of patient spinal cord tissues revealed evidence of severe myelin loss restricted to the posterior spinal funiculus in Patients 3 and 12. This myelin loss was present throughout all spinal levels demonstrated by Loyez stain and myelin basic protein immunohistochemistry in Patient 3 (Fig. 1D and G) with more profound loss in the fasciculus gracilis than cuneatus. This was in contrast to control spinal cord, which showed uniform myelin staining (Fig. 1A). The extreme disparity between a normally myelinated region, such as the anterior

Table 2 Neuronal cell density in spinal cord and dorsal root ganglion tissues from Patient 3 and age-matched controls

	Patient 3	Controls
Dorsal root ganglia	5.75 ± 0.98	14.00 ± 4.86 (n = 2)
Posterior horn cell	15.15 ± 11.43	38.40 ± 16.42 (n = 3)
Anterior horn cell	21.84 ± 4.63	35.48 ± 25.57 (n = 3)

Neuronal cell density (neurons/mm^2 ± standard deviation) is reduced in Patient 3 versus control in the dorsal root ganglion and in the posterior horn of spinal cord; this is a statistically significant observation (dorsal root ganglia: P = 0.0111 and posterior horn: P = 0.0039). The reduction in neuronal density in the anterior horn is not statistically significant.

funiculus, and the demyelinated posterior funiculus is exemplified in Fig. 1H and I. In addition, there is a profound loss of axons in the corresponding regions of myelin loss in patient tissues (Fig. 1E and F) in comparison with controls (Fig. 1B and C). In contrast to the severe loss of axons and myelin in the posterior funiculus, evaluation of the oligodendrocytic marker, CNPase, showed relatively intact density of the CNS myelinating cells in this region (Fig. 1J, K and L).

Quantitation of neuronal cell density

Quantitative assessment of neuronal cell density within the dorsal root ganglia and spinal cord grey matter of Patient 3 revealed that neuronal density was reduced in patient tissues (Table 2). The reduction was statistically significant in the dorsal root ganglia with 5.75 neurons/mm^2 ± 0.98 standard deviations (SD) relative to 14.00 neurons/mm^2 ± 4.86 SD in two age-matched controls (unpaired t-test with Welch's correction, P = 0.0111; Table 2 and shown in Fig. 2A and B). In addition, the patient dorsal root ganglia neurons were much smaller (1935 μm^2 ± 815.2 SD) in comparison with control neurons (2655 μm^2 ± 993.7 SD; Mann–Whitney test, P = 0.018). Statistically significant reduction was also present in the posterior horn interneuron population with a cell density of 15.15 neurons/mm^2 ± 11.43 SD relative to 38.40 neurons/mm^2 ± 16.42 SD in three age-matched controls (unpaired t-test with Welch's correction, P = 0.0039). There was also some neuron loss in the anterior horn of the patient (21.84 neurons/mm^2 ± 4.63 SD) relative to controls (35.48 neurons/mm^2 ± 25.57 SD) but this was not statistically significant.

Mitochondrial respiratory chain deficiency

Analysis of the expression of mitochondrial respiratory chain proteins was performed in spinal cord tissues to determine the extent of the respiratory deficiency. Porin immunohistochemistry revealed a comparable distribution and density of mitochondria in control and patient spinal cord neurons. Complex I immunohistochemistry showed diffuse deficiency for subunits 20 kDa, 30 kDa and 39 kDa in the patient posterior horn neurons, suggesting that complex I activity was diminished in this region. Complex IV subunit expression and activity was intact in all posterior horn neurons, as judged by mitochondrially encoded complex IV subunit I (COX-I) immunohistochemistry and COX/succinate dehydrogenase histochemistry.

In contrast to the spinal cord, Patient 3 dorsal root ganglia neurons exhibited abnormal mitochondrial morphology and dysfunction. Porin immunohistochemistry revealed an unusual cytoplasmic distribution and density of mitochondria in patient neurons compared with age-matched controls (Fig. 2C and D). Mitochondrial mass varied between neurons showing normal distribution but others showing low mitochondrial density (Fig. 2D). The reduction in mitochondrial mass was confirmed by complex II 70 kDa immunohistochemistry and succinate dehydrogenase histochemistry (Figs. 2H and 3C–E). Immunohistochemistry demonstrated reduced expression of protein subunits comprising complexes I and IV of the respiratory chain in Patient 3 dorsal root ganglia neurons. Complex I expression was reduced in approximately one-third of the neuronal population with 33% and 34% of neurons exhibiting deficiency for subunits 15 and 20 kDa, respectively (Fig. 2E and F). Assessment of complex IV demonstrated reduced protein expression of the mitochondrially-encoded subunit I (COX-I) and nuclear-encoded subunit IV (COX-IV) relative to control neurons (Fig. 2J–M). Biochemically, the dorsal root ganglia neuronal population were 60% COX-deficient, which is a higher level of deficiency relative to COX-I protein (Fig. 3A). It is important to note here that, whereas control dorsal root ganglia neurons demonstrated mild respiratory deficiency for complex I, this was only present at low levels (<5%) and deficiency was not detected by COX/succinate dehydrogenase histochemistry.

Molecular genetic investigation in the dorsal root ganglia

We next determined the level of mitochondrial DNA deletion in COX-deficient and COX-positive neurons from Patient 3 to establish whether a causal relationship exists (Fig. 3B). The mean percentage level of mitochondrial DNA deletion was higher (34.08%) in COX-deficient neurons relative to COX-positive neurons (19.02%), however, this was not statistically significant (Mann–Whitney test, P = 0.08). A small number of COX-deficient neurons did have high levels of mitochondrial DNA deletion; however, in many neurons the low level of mitochondrial DNA deletion detected is insufficient alone to cause the observed respiratory chain deficiency.

Next, we evaluated mitochondrial DNA copy number in 30 succinate dehydrogenase-positive dorsal root ganglia neurons from Patient 3 and 19 neurons from control using both the *MT-ND1* and *MT-ND4* genes as a reference; *MT-ND1* is used to measure absolute mitochondrial DNA copy number since it is rarely deleted, whereas *MT-ND4* is often deleted in the presence of clonally expanded mitochondrial DNA deletions and can therefore be used to determine the relative amount of wild-type mitochondrial DNA present in a single cell using this assay (Krishnan *et al*., 2007). Succinate dehydrogenase staining was used because previous results showed interference of the 3,3′-diaminobenzadine deposit in the COX reaction with real-time polymerase chain reaction. The overall *MT-ND1* copy number was dramatically decreased in patient dorsal root ganglia neurons relative to control dorsal root ganglia neurons (Fig. 3F; Mann–Whitney test, P = 0.003), inferring that not only do these neurons harbour mitochondrial DNA

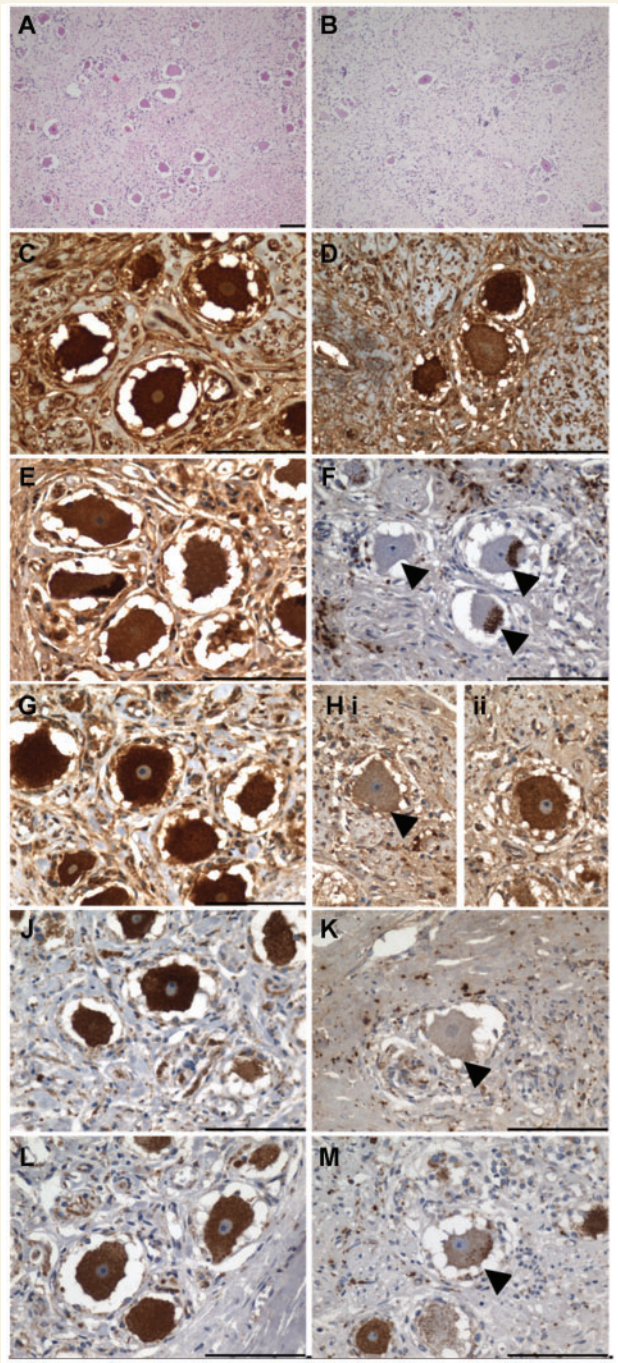

Figure 2 Dorsal root ganglia in Patient 3 display prominent reduction in sensory neuron density and respiratory chain deficiency. Relative to control (**A**) neuronal cell density in Patient 3 (**B**) is significantly reduced (unpaired *t*-test with Welch's correction, $P = 0.0111$). (**C**) Control dorsal root ganglia: neurons demonstrate uniformly high expression of porin indicating mitochondrial mass is high in these neurons (porin immunohistochemistry). (**D**) Patient dorsal root ganglia: level of cytoplasmic porin expression is variable, with a number of neurons demonstrating a reduced mass of mitochondria. (**E**) Control dorsal root ganglia: uniformly high cytoplasmic levels of subunit 15 kDa of complex I in neurons. (**F**) Patient dorsal root ganglia: neurons show profound loss of complex I subunit 15 kDa with small foci of abnormal clustering of immunoreactivity in the neuronal cell body (arrowheads). (**G**) Control dorsal root ganglia: uniformly high level of complex II 70 kDa expression throughout the neuronal population. (**H**) Patient dorsal root ganglia: neurons demonstrate variability in expression with some neurons demonstrating decreased expression [**H(i)**, arrowhead] and others with intact expression [**H(ii)**]. (**J**) Control dorsal root ganglia: neurons demonstrate uniformly high level of COX-I expression. (**K**) Patient dorsal root ganglia: profound COX-I deficiency in neurons (arrowhead). (**L**) Control dorsal root ganglia: neuronal COX-IV expression is also intact. (**M**) Patient dorsal root ganglia: evidence of neuronal COX-IV deficiency (arrowhead). Scale bars = 100 μm.

deletions, but that they also contain a lower absolute mitochondrial DNA copy number indicative of a quantitative mitochondrial DNA depletion. Evaluation of *MT-ND4* levels showed a pronounced loss of wild-type mitochondrial DNA in patient neurons (Fig. 3G; Mann–Whitney test, $P < 0.0001$), which is consistent with the presence of mitochondrial DNA deletions in these cells. However, overall mitochondrial DNA depletion is likely to be the main mediator driving development of respiratory chain deficiency in dorsal root ganglia neurons.

Discussion

Since peripheral neuronopathy is a common, yet poorly understood, neurological symptom in patients with *POLG* mutations, this study aimed to elucidate the molecular mechanisms underpinning PNS dysfunction. Here, we describe the electrophysiological findings from 11 patients with autosomal recessive *POLG* mutations and perform a detailed neuropathological investigation on two patients. Our results confirm that peripheral neuronopathy is an important clinical symptom in patients harbouring autosomal recessive *POLG* mutations. Electrophysiological assessment typically reveals a sensory neuronopathy with motor fibre involvement developing later in the course of the disease. In our cases, motor fibre involvement tended to remain relatively mild, suggesting a greater vulnerability of sensory neurons and their projections. This is entirely compatible with previous reports where electrophysiological assessment of patients harbouring *POLG* mutations points to sensory neuronopathy due to the absence of sensory nerve action potentials with normal or minimally reduced conduction velocity (Van Goethem *et al*., 2004; Hakonen *et al*., 2005; Tzoulis *et al*., 2006; Schulte *et al*., 2009; McHugh *et al*., 2010; Weiss and Saneto, 2010). Generally, normal motor nerve conduction is observed, however, a small number of patients demonstrate reduced motor nerve conduction velocities (Schulte *et al*., 2009).

Although we have clarified the electrophysiological features of peripheral neuronopathy in POLG deficiency there is limited neuropathological information about the aetiology of this disorder. Previous post-mortem studies report a generalized degeneration of the posterior spinal funiculus in patients with mitochondrial disease, not just restricted to those harbouring *POLG* defects (Cottrell *et al*., 2000; Horvath *et al*., 2006; Hopkins *et al*., 2010).

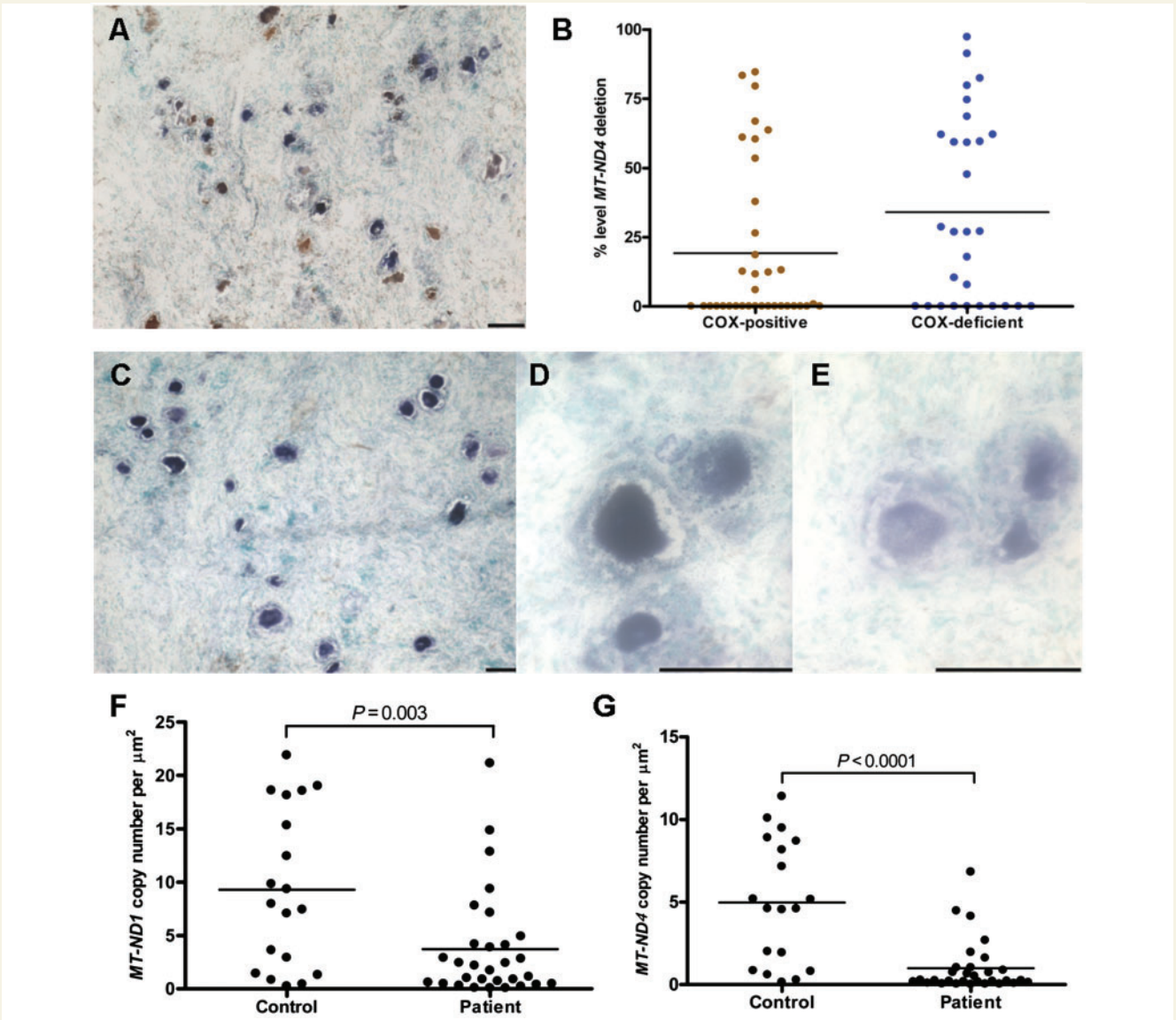

Figure 3 High levels of COX-deficiency, presence of mitochondrial DNA deletions and evidence of reduced mitochondrial DNA copy number in Patient 3 dorsal root ganglia neurons. (**A**) Patient COX/succinate dehydrogenase histochemistry reveals 60% neuronal COX-deficiency (COX/succinate dehydrogenase histochemistry, blue cells). (**B**) Molecular analysis of patient dorsal root ganglia tissues shows the mean level of mitochondrial DNA deletions is slightly higher in COX-deficient neurons versus COX-positive neurons. (**C**) Succinate dehydrogenase histochemistry on patient dorsal root ganglia neurons reveals some variability in activity between neurons (succinate dehydrogenase histochemistry), with some neurons demonstrating a high level of succinate dehydrogenase activity (**D**) and some with only a low level of succinate dehydrogenase activity (**E**). (**F**) *MT-ND1* copy number: evidence of mitochondrial DNA depletion is shown by a significant reduction in absolute copy number with *MT-ND1* in patient neurons relative to controls (Mann–Whitney test, $P = 0.003$). (**G**) *MT-ND4* copy number: wild-type mitochondrial DNA copy number, as assessed by *MT-ND4,* is significantly lower in patient neurons relative to control neurons (Mann–Whitney test, $P < 0.0001$), indicative of presence of mitochondrial DNA deletions in the patient's dorsal root ganglia neurons.

Rantamaki and colleagues (2001) reported evidence of slight degeneration and atrophy of the dorsal root ganglia associated with fibre depletion from the posterior spinal cord in a patient later reported to harbour *POLG* mutations (Rantamaki *et al*., 2001; Van Goethem *et al*., 2004; Hakonen *et al*., 2005). Our study provides evidence in support of posterior spinal funiculus degeneration with evidence of severe axonal and myelin loss and sensory neuron degeneration in two patients with autosomal recessive *POLG* mutations. We have explored this in further detail to document the neurodegenerative changes taking place in the dorsal root ganglia and spinal column neuronal populations. We show significantly reduced neuronal density suggestive of cell loss in the dorsal root ganglia and posterior horn neuronal populations. Evidence of mitochondrial dysfunction can be clearly observed in the remaining neurons within the dorsal root ganglia with profound respiratory deficiency involving complexes I and IV.

We propose that the commonly observed posterior funiculus degeneration and posterior horn cell loss are secondary phenomena caused by sensory neuronal dysfunction and death in the dorsal root ganglia leading to a loss of their central axonal branches/ascending fibres in the posterior funiculus and posterior horn neurons within the spinal cord. This has been highlighted by the remarkable loss of axons and the subsequent loss of myelin from the posterior spinal funiculus and reduced interneuron density in the posterior horn. The predominantly sensory peripheral neuronopathy commonly observed in patients with *POLG* mutations is likely due to loss of the peripheral axonal branches of the dorsal root ganglia neurons, secondary to the death of the dorsal root ganglia neurons.

Since high levels of respiratory-deficient neurons were seen in dorsal root ganglia neurons, molecular analysis was performed to establish the cause of deficiency. Since adult patients who harbour *POLG* mutations often acquire multiple mitochondrial DNA deletions (Van Goethem *et al*., 2001, 2004), the percentage levels of mitochondrial DNA deletions were determined in dorsal root ganglia COX-positive and COX-deficient neurons. In the patient examined in this study, many COX-deficient neurons had low levels of mitochondrial DNA deletion indicating other factors important in the development of a biochemical defect. Mitochondrial DNA copy number analysis showed dorsal root ganglia neurons with a dramatically reduced *MT-ND4* and *MT-ND1* copy number suggestive of not only a decrease in number of wild-type mitochondrial DNA copies, but absolute mitochondrial DNA copy number. This finding was also supported by immunohistochemical assessment of mitochondrial density that revealed prominent changes in the mitochondrial distribution throughout the population of dorsal root ganglia neurons. Mitochondrial DNA depletion is described in association with recessive *POLG* mutations, however, this is in the context of early-onset and severe cases of mitochondrial disease including Alpers–Huttenlocher syndrome and infantile hepatocerebral presentations (Stewart *et al*., 2009). We believe that this quantitative loss of mitochondrial DNA is likely to be important in the pathophysiological process of the neurodegeneration observed in these adult cases, given the correlation with the altered mitochondrial mass as determined histochemically in dorsal root ganglia neurons.

Our study confirms that peripheral neuronopathy in patients with autosomal recessive *POLG* mutations primarily arises due to a dorsal root ganglionopathy. This is an important contributor to morbidity and reduced quality of life in these patients and unfortunately there is no successful treatment. We do not know why the dorsal root ganglia neurons are particularly susceptible to *POLG* mutations but perhaps, we can speculate that this relates to the metabolic activity of these neurons. An increasing number of mitochondrial defects are being identified in patients with peripheral neuronopathies (Zuchner *et al*., 2004) and it is important to explore the mechanisms involved.

Acknowledgements

Additional tissue was provided by the Sheffield Brain Tissue Bank.

Funding

Tissue for this study was provided by the Newcastle Brain Tissue Resource, which is funded in part by a grant from the UK Medical Research Council (G0400074). This work was supported by The Wellcome Trust (074454/Z/04/Z); the Newcastle University Centre for Brain Ageing and Vitality supported by BBSRC, EPSRC, ESRC and MRC as part of the cross-council Lifelong Health and Wellbeing Initiative (G0700718); UK NIHR Biomedical Research Centre for Ageing and Age-related disease award to the Newcastle upon Tyne Hospitals NHS Foundation Trust; the UK NHS Specialist Commissioners, which funds the 'Rare Mitochondrial Disorders of Adults and Children' Diagnostic Service in Newcastle upon Tyne (http://www.mitochondrialncg.nhs.uk).

Supplementary material

Supplementary material is available at *Brain* online.

References

Betts J, Jaros E, Perry RH, Schaefer AM, Taylor RW, Abdel-All Z, et al. Molecular neuropathology of MELAS: level of heteroplasmy in individual neurones and evidence of extensive vascular involvement. Neuropath Appl Neurobiol 2006; 32: 359–73.

Clayton DA. Replication of animal mitochondrial DNA. Cell 1982; 28: 693–705.

Cottrell DA, Ince PG, Blakely EL, Johnson MA, Chinnery PF, Hanna M, et al. Neuropathological and histochemical changes in a multiple mitochondrial DNA deletion disorder. J Neuropathol Exp Neurol 2000; 59: 621–7.

Deschauer M, Tennant S, Rokicka A, He L, Kraya T, Turnbull DM, et al. MELAS associated with mutations in the *POLG1* gene. Neurology 2007; 68: 1741–2.

Fadic R, Russell JA, Vedanarayanan VV, Lehar M, Kuncl RW, Johns DR. Sensory ataxic neuropathy as the presenting feature of a novel mitochondrial disease. Neurology 1997; 49: 239–45.

Filosto M, Mancuso M, Nishigaki Y, Pancrudo J, Harati Y, Gooch C, et al. Clinical and genetic heterogeneity in progressive external ophthalmoplegia due to mutations in polymerase gamma. Arch Neurol 2003; 60: 1279–84.

Gago MF, Rosas MJ, Guimaraes J, Ferreira M, Vilarinho L, Castro L, et al. SANDO: two novel mutations in *POLG1* gene. Neuromuscul Disord 2006; 16: 507–9.

Hakonen AH, Heiskanen S, Juvonen V, Lappalainen I, Luoma PT, Rantamaki M, et al. Mitochondrial DNA polymerase W748S mutation: a common cause of autosomal recessive ataxia with ancient European origin. Am J Hum Genet 2005; 77: 430–41.

He L, Chinnery PF, Durham SE, Blakely EL, Wardell TM, Borthwick GM, et al. Detection and quantification of mitochondrial DNA deletions in individual cells by real-time PCR. Nucleic Acids Res 2002; 30: e68.

Hopkins SE, Somoza A, Gilbert DL. Rare autosomal dominant *POLG1* mutation in a family with metabolic strokes, posterior column spinal degeneration, and multi-endocrine disease. J Child Neurol 2010; 25: 752–6.

Horvath R, Hudson G, Ferrari G, Futterer N, Ahola S, Lamantea E, et al. Phenotypic spectrum associated with mutations of the mitochondrial polymerase gamma gene. Brain 2006; 129: 1674–84.

Krishnan KJ, Bender A, Taylor RW, Turnbull DM. A multiplex real-time PCR method to detect and quantify mitochondrial DNA deletions in individual cells. Anal Biochem 2007; 370: 127–9.

McHugh JC, Lonergan R, Howley R, O'Rourke K, Taylor RW, Farrell M, et al. Sensory ataxic neuropathy dysarthria and ophthalmoparesis (SANDO) in a sibling pair with a homozygous p.A467T *POLG* mutation. Muscle Nerve 2010; 41: 265–9.

Naviaux RK, Nguyen KV. *POLG* mutations associated with Alpers' syndrome and mitochondrial DNA depletion. Ann Neurol 2004; 55: 706–12.

Rantamaki M, Krahe R, Paetau A, Cormand B, Mononen I, Udd B. Adult-onset autosomal recessive ataxia with thalamic lesions in a Finnish family. Neurology 2001; 57: 1043–9.

Schicks J, Synofzik M, Schulte C, Schols L. *POLG*, but not PEO1, is a frequent cause of cerebellar ataxia in Central Europe. Mov Disord 2010; 25: 2678–82.

Schulte C, Synofzik M, Gasser T, Schols L. Ataxia with ophthalmoplegia or sensory neuropathy is frequently caused by *POLG* mutations. Neurology 2009; 73: 898–900.

Stewart JD, Tennant S, Powell H, Pyle A, Blakely EL, He L, et al. Novel *POLG1* mutations associated with neuromuscular and liver phenotypes in adults and children. J Med Genet 2009; 46: 209–14.

Stricker S, Pruss H, Horvath R, Baruffini E, Lodi T, Siebert E, et al. A variable neurodegenerative phenotype with polymerase gamma mutation. J Neurol Neurosurg Psychiatry 2009; 80: 1181–2.

Taylor RW, Barron MJ, Borthwick GM, Gospel A, Chinnery PF, Samuels DC, et al. Mitochondrial DNA mutations in human colonic crypt stem cells. J Clin Invest 2003; 112: 1351–60.

Tzoulis C, Engelsen BA, Telstad W, Aasly J, Zeviani M, Winterthun S, et al. The spectrum of clinical disease caused by the A467T and W748S *POLG* mutations: a study of 26 cases. Brain 2006; 129: 1685–92.

Van Goethem G, Dermaut B, Lofgren A, Martin JJ, Van Broeckhoven C. Mutation of *POLG* is associated with progressive external ophthalmoplegia characterized by mtDNA deletions. Nat Genet 2001; 28: 211–2.

Van Goethem G, Luoma P, Rantamaki M, Al Memar A, Kaakkola S, Hackman P, et al. *POLG* mutations in neurodegenerative disorders with ataxia but no muscle involvement. Neurology 2004; 63: 1251–7.

Van Goethem G, Martin JJ, Dermaut B, Lofgren A, Wibail A, Ververken D, et al. Recessive *POLG* mutations presenting with sensory and ataxic neuropathy in compound heterozygote patients with progressive external ophthalmoplegia. Neuromuscul Disord 2003; 13: 133–42.

Weiss MD, Saneto RP. Sensory ataxic neuropathy with dysarthria and ophthalmoparesis (SANDO) in late life due to compound heterozygous *POLG* mutations. Muscle Nerve 2010; 41: 882–5.

Winterthun S, Ferrari G, He L, Taylor RW, Zeviani M, Turnbull DM, et al. Autosomal recessive mitochondrial ataxic syndrome due to mitochondrial polymerase gamma mutations. Neurology 2005; 64: 1204–8.